Chemical Science

Accepted Manuscript

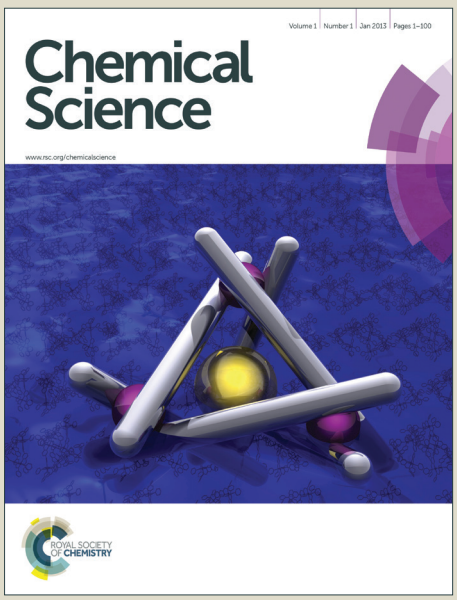

ROYAL SOCIETY OF CHEMISTRY

www.rsc.org/chemicalscience

Journal Name

RSCPublishing

ARTICLE

Mass preparation of high-quality graphene from glucose and ferric chloride

Cite this: DOI: 10.1039/x0xx00000x

Binbin Zhang, Jinliang Song*, Guanying Yang, Buxing Han*

Received 00th January 2012,
Accepted 00th January 2012

DOI: 10.1039/x0xx00000x

www.rsc.org/

Graphene and its derivatives have great potential of applications. Mass preparation of high-quality graphene by simple methods using cheap feedstocks is crucial for its wide applications. Glucose is abundant and renewable carbon resource and $FeCl_3$ is a very cheap salt. Herein we proposed a new method to prepare graphene, which composed simply of dissolution of glucose and $FeCl_3$ in water, vaporization of water, and calcination. It was found that graphene up to few layers could be prepared and their electrical conductivity was similar to that of the graphene sheets synthesized from chemical vapor deposition (CVD) method. Further study indicated that $FeCl_3$ was the key to the generation of high-quality graphene because it acted as both template and catalyst for the formation of graphene.

Introduction

Graphene has attracted extensive attention since the fabrication of mono-layer graphene through mechanical exfoliation of graphite in 2004.[1] Graphene and graphene-based materials have great potential of application in different fields such as physics, material science, and chemistry due to its outstanding electronic,[1, 2] mechanical,[3] optical,[4] and thermal[5] properties.

Different methods have been developed to generate graphene,[6] and each of them has advantages and disadvantages. For example, single sheet of pristine graphene in small amounts was obtained by micromechanical exfoliation of graphite.[1] Both mono-layer and multi-layer graphene have been produced by the chemical vapor deposition (CVD) of hydrocarbons on different substrates,[7] substrate-free deposition[8] or by epitaxial growth on SiC.[9] Exfoliation of graphite in solvents is another method to fabricate graphene.[10] A drawback of this method is its low yield efficiency and long sonication time,[11] which is energy-intensive and usually leads to the destruction of graphene. Addition of intercalants in the solution can increase the concentration of graphene, but this introduces impurity. Oxidation-reduction method,[12] which comprises oxidation of graphite to graphene oxide (GO) followed by chemical reduction to generate reduced GO (rGO), can achieve mass production of graphene material with low cost, but the resultant graphene sheets contain high levels of defects and oxygen content. Graphene sheets can also be prepared by pyrolysis or calcination methods using different carbon sources.[13] In addition, graphene materials can be synthesized by solvothermal method.[12a, 14] In general, mechanical exfoliation and CVD methods can produce high-quality graphene, but it is very difficult for mass preparation using these approaches. Oxidation-reduction, pyrolysis, calcination, and solvothermal methods can be used to prepare larger amount of graphene materials, but it is very difficult to fabricate high-quality products using these methods.

Development of simple methods to prepare high-quality graphene sheets in large scale is highly desirable, but is challenging. In this work, we report the successful mass preparation of high-quality graphene sheets simply by carbonization and calcination of glucose and $FeCl_3$ mixture. It was demonstrated that $FeCl_3$ was essential to obtain the high-quality of graphene material. This novel and simple method for mass preparation of graphene sheets with relative high-quality benefits large-scale applications of graphene in different fields.

Results and discussion

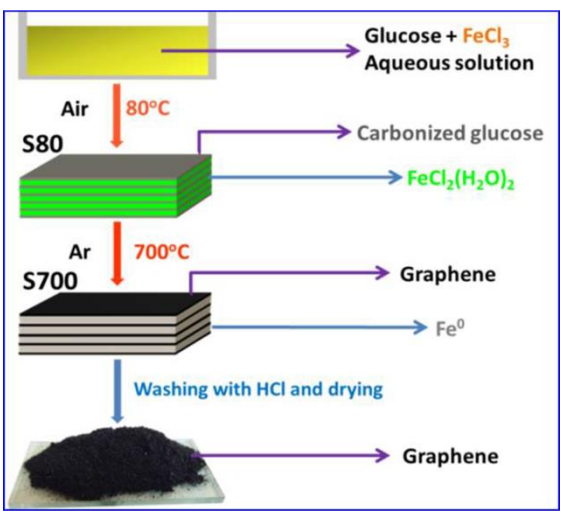

Fig. 1. Schematic diagram for the synthesis of graphene sheets through carbonization and calcination of glucose and $FeCl_3$ mixture.

The procedures to prepare the graphene sheets are illustrated schematically in Fig. 1. Glucose and $FeCl_3$ were firstly dissolved in water to form a yellow aqueous solution. The solution was evaporated at 80 ^oC in air and carbonized glucose (S80) was formed. Then the S80 was calcined at 700 ^oC under Argon flow to generate graphene/iron composite (S700). The iron in the as-prepared S700 was removed by HCl aqueous solution, and the graphene sheets were obtained after washing with solvents and drying.

Raman spectroscopy is a commonly used technique for characterization of graphene materials.[15] In the Raman spectrum of a typical graphene material, D-band (~1350 cm^{-1}), G-band (~1570 cm^{-1}) and 2D-band (~2675 cm^{-1}) are the three main characteristic bands. The G-band gives the evidence for the existence of sp^2-hybridized carbon atoms, and the D-band demonstrates defects such as disorder, edges and boundaries of the graphene. The 2D-band provides information of the number of layers of the graphene material. The relative intensities of the G-band (I_G), D-band (I_D), and 2D-band (I_{2D}) provide evidence for studying the characteristics of graphene materials. Graphene materials with high quality have low I_D/I_G ratio and high I_{2D}/I_G ratio.

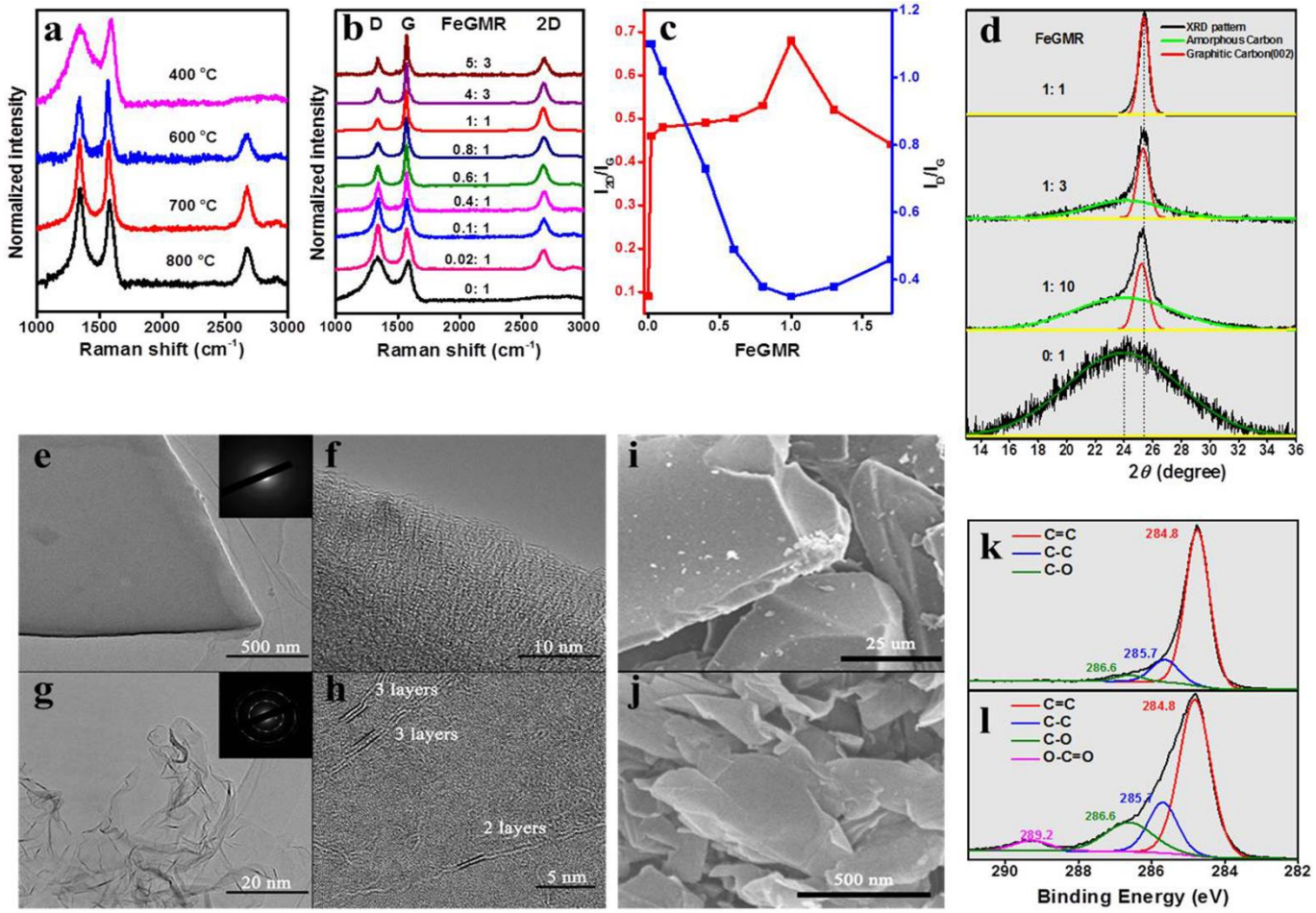

Fig. 2. Characterization of the materials. (a) Raman spectra of the samples prepared by calcination of the S80 at different temperatures (FeGMR=1:10). (b) Raman spectra of the materials prepared using the feedstocks with different FeGMRs by calcination of S80 at 700 ^oC. (c) I_{2D}/I_G and I_D/I_G values of the materials prepared using the feedstocks with different FeGMRs by calcination of S80 at 700 ^oC. (d) XRD patterns of the graphite materials prepared using the feedstocks with different FeGMRs by calcination of S80 at 700 ^oC. The lamellar repeat period of the graphite material prepared using the feedstock with 1:1 FeGMR was 0.340 Å as calculated from the patterns. (e) TEM image of the material prepared without $FeCl_3$ by calcination of S80 at 700 ^oC and the corresponding SAED pattern (inset). (f) The magnified TEM image of the edge of the plate in e. (g) TEM image of the material prepared using the feedstock with 1:1 FeGMR and the corresponding SAED pattern (inset), and the image illustrates the rolling and folded structure in some areas. (h) The TEM image of the edges of the graphene sheets in g, showing the bilayer and tri-layer structures. (i) SEM image of the material prepared without $FeCl_3$by calcination of S80 at 700 ^oC. (j) SEM image of the material prepared using the feedstock with 1: 1 FeGMR by calcination of S80 at 700 ^oC. (k) XPS spectra of the graphite material prepared using the feedstock with 1:1 FeGMR by calcination of S80 at 700 ^oC. (l) XPS spectra of the material prepared using the feedstock without $FeCl_3$ by calcination of S80 at 700 ^oC.

Journal Name RSCPublishing

ARTICLE

The Raman spectra (532 nm Laser excitation) of the samples prepared by calcination of the S80 with $FeCl_3$ to glucose mass ratio (FeGMR) 1:10 at different temperatures are given in Fig. 2a. The results indicated that the graphene obtained at 700 ^oC had the highest quality. The Raman spectra of the materials prepared using the feedstocks with different FeGMRs are presented in Fig. 2b, and Fig. 2c illustrates the dependence of the I_{2D}/I_G and I_D/I_G ratios on the FeGMR. $FeCl_3$ affected the I_{2D}/I_G and I_D/I_G ratios significantly. When neat glucose was used without $FeCl_3$, the D-band is strong, while the 2D band is very weak, indicating that amorphous carbon structure is dominant,[13c] *i.e*, the quality of the graphite material was very poor in the absence of $FeCl_3$. Fig. 2c shows that the I_D/I_G value decreased with increasing $FeCl_3$ content at beginning, and reached a minimum as the FeGMR was 1:1. At this FeGMR, the I_D/I_G value of the graphene sheets was 0.35, which is much smaller than that of a typical rGO (usually >1).[16] This indicated that the graphene flakes of high-quality could be prepared using the method proposed in this work. The defects may predominantly locate at the edges of the graphene flakes.[17] This conclusion is also supported by the fact that the electrical conductivity of the sample determined in this work was 768 S/m, which is similar to that of the graphene with an average number of three layers prepared by CVD method.[18] With increasing $FeCl_3$ content in the feedstock, the I_{2D}/I_G value increased dramatically at the beginning, then increased slowly, and reached maximum at 1:1 FeGMR, demonstrating that the graphene prepared at this condition had least layers. The I_{2D}/I_G was 0.68, suggesting the character of graphene sheets with about 3 layers.[15a] The above results indicate that the graphene prepared at 1:1 FeGMR by calcination of S80 at 700 ^oC had highest quality, and the graphene yield was 40 % calculated based on the added carbon in the glucose.

X-ray diffraction (XRD) patterns (Fig. 2d) further revealed the crucial role of $FeCl_3$ in the conversion of glucose to high-quality graphene. The pattern of the material prepared without $FeCl_3$ demonstrated a broad peak at about 2θ=24 degree corresponding to amorphous carbon,[19] and the peak at about 2θ=26 degree corresponding to (002) plane of graphite carbon[19,20] was not observable. With increasing the content of $FeCl_3$ in the feedstock, the intensity of the peak of the amorphous carbon decreased and that of the graphite carbon increased. At the 1:1 FeGMR, the peak of amorphous carbon disappeared and only the strong peak at about 2θ=26 degree was observed. The results indicate that the graphene sheets prepared at this condition had highest quality, and the conclusion was consistent with that derived from Raman spectroscopy study.

Representative transmission electron microscopy (TEM) images of the typical materials are shown in Figs. 2e-2h. Figs. 2e and 2f are the images of the material prepared using glucose without $FeCl_3$. The material had thick plate morphology, and the corresponding selected area electron diffraction (SAED) pattern (inset) revealed the character of amorphous carbon (Fig. 2e). Fig. 2f is the enlarged image of the edge of the plate in Fig. 2e. Graphene-layered structure could not be observed, which confirmed its amorphous structure of the material prepared without using $FeCl_3$. Figs. 2g and 2h are the images of the materials prepared using the feedstock with 1:1 FeGMR. Fig. 2g demonstrates the graphene sheets, and some areas had rolled and folded structures because the films were very thin. The SAED pattern (inset) in Fig. 2g indicates that the graphene sheets were crystalline. Fig. 2h shows the fine structure at the edges of the graphene. The as-synthesized graphene sheets were composed mainly of graphene sheets up to few layers. This agrees with the conclusion obtained from Raman spectroscopy study.

The scanning electron microscopy (SEM) images of some typical materials are given in Figs. 2i and 2j. The material fabricated without $FeCl_3$ (FeGMR=0:1) had bulk morphology (Fig. 2i). The graphene material prepared with 1:1 FeGMR showed sheet morphology (Fig. 2j). X-ray photoelectron spectroscopy (XPS) was applied to study the samples prepared by calcination of the S80 with and without $FeCl_3$ at 700 ^oC, and the results are presented in Figs. 2k and 2l. The intensity ratio between sp^2-hybridized C=C bond at 284.8 eV[21] and sp^3-hydridized C-C bond at 285.7 eV[22] for the graphene sheets prepared with the feedstock of 1:1 FeGMR is 5.8 (Fig. 2k), while the ratio is only 2.8 (Fig. 2l) for the sample fabricated without $FeCl_3$. In addition, the sample fabricated without $FeCl_3$ contains considerable amounts of C-O and O-C=O bonds (Fig. 2l), which correspond to binding energies of 286.6 eV and 289.2 eV, respectively.[22]

As discussed above, $FeCl_3$ played a key role in the preparation of the high-quality graphene sheets. We carried out more experiments using the feedstock with 1:1 FeGMR to explain this phenomenon. XRD study (Fig. 3a) indicated that the iron salt in the S80 (Fig. 1) existed in the form of $FeCl_2(H_2O)_2$ crystals. The Fe contents of the S80 determined by XPS and ICP studies were 15.4 wt% and 39.0 wt%, respectively. This indicated uneven distribution of Fe in the S80 because XPS reflects the composition at the surface, while ICP technique gives the overall composition. SEM study indicated that the S80 had a layered structure (Fig. 3b). It can be deduced that $FeCl_2(H_2O)_2$ layers and carbonized glucose layers existed alternatively in the S80, and the outer layers were the carbonized glucose. ICP analysis indicated that the S80 contained 40 wt% C, 52.6 wt% O, and 7.4 wt% H on the iron salt-free basis. XRD study (Fig. 4a) demonstrated that the Fe^{2+} in the S80 was reduced to Fe^0 during the calcination at 700 ^oC under Argon flow to form the S700. This argument was further supported by the fact that the S700 could be attracted by a magnet (Figs. 4b and 4c), and that H_2 gas was generated during washing the S700 with HCl aqueous solution. SEM study showed that the S700 also had layered structure (Fig. 4d). Iron contents of the S700 determined by XPS and ICP techniques were 1.0 wt% and 41.1 wt%, respectively. This also suggests that the graphene layers and Fe^0 layers existed alternatively in the S700, and the outer layers were graphene. The existence of the Fe^0 sheets in the S700 was further confirmed by the fact that the iron residue remained sheet morphology after removing the carbon in the air at 600 ^oC for 1 hour (Fig. 4e). In addition, ICP analysis indicated that the graphene contained 98.5 wt% C, 1.5 wt% H, and O was not negligible, illustrating that most of the H

and O atoms in the S80 were removed during the calcination of the S80 at 700 °C.

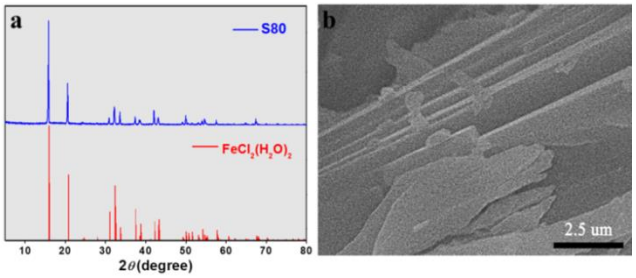

Fig. 3. Characterization of the S80 prepared using the feedstock with 1:1 FeGMR. (a) Standard XRD pattern of $FeCl_2(H_2O)_2$ (bottom) and the XRD pattern of the S80 (top). (b) The SEM image of the S80.

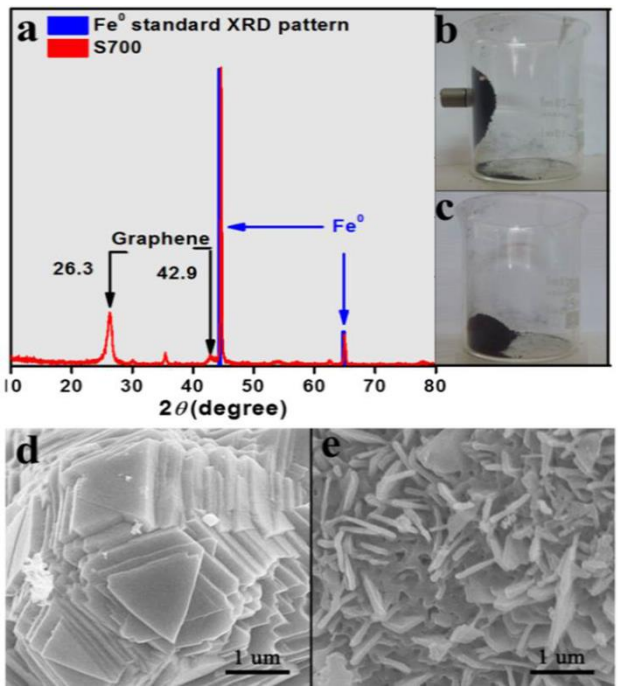

Fig. 4. Characterization of the S700 prepared by calcination of the S80 at 700 °C using the feedstock with 1:1 FeGMR. (a) XRD pattern of the S700. (b) and (c) Photos of the sample attracted by a magnet and after removing the magnet. (d) The SEM image of the S700. (e) The SEM image of the S700 after removing the carbon at 600 °C in air for 1 hour.

On the basis of the results above we propose the pathway and mechanism for the formation of the graphene sheets, which is discussed in combination with Fig. 1. An aqueous solution is formed after the dissolution of glucose and $FeCl_3$ in water. A sandwich-like composite (S80) with the carbonized glucose layers and $FeCl_2(H_2O)_2$ layers is formed during the vaporization of water in the aqueous solution of glucoses and $FeCl_3$ in the air. The Fe^{2+} in the S80 is reduced to Fe^0 during the calcination at 700 °C under protection of Argon. It is well known that Fe^0 is a commonly used catalyst in the preparation of carbon nanotubes from carbon materials.[23] Similarly, the in-situ formed Fe^0 sheets serve both as the template and the catalyst for the formation of graphene sheets. Therefore, high quality graphene sheets are formed, and can be obtained after removing the iron by washing with HCl aqueous solution.

Conclusion

In summary, high-quality graphene sheets can be synthesized by a simple route that is composed of dissolution of glucose and $FeCl_3$ in water, vaporization of water in the air, and calcination at higher temperature. The $FeCl_3$ plays key role for the generation of the high-quality graphene because it acts as both template and catalyst for the formation of graphene. Graphene sheets up to few layers can be prepared easily by this method and their electrical conductivity is similar to that of the graphene sheets synthesized from CVD method. The simple, greener, and cheaper protocol opens a new way for mass preparation of high-quality graphene flakes.

Experimental

Chemicals

Anhydrous glucose (A. R. grade) and anhydrous $FeCl_3$ (A. R. grade) were purchased from Alfa Aesar China Co., Ltd. The Ar (99.99%) was provided by Beijing Analytical Instrument Company. Double distilled water was used in all of the experiments.

Preparation of graphene materials

In a typical experiment, 3 g glucose and desired amount of $FeCl_3$ were dissolved in 5 mL water in a porcelain boat. The yellow colored solution was vaporized at 80 °C in air in an oven for 24 hours, and black solid (S80) was obtained. The S80 was calcined in a quartz tube furnace at suitable temperature for 6 hours with an Argon flow of 20 mL/min. Then, the furnace was cooled down to room temperature under protection of Argon flow. After that, the sample was placed in a beaker containing 50 mL hydrochloric acid (36 wt%) with magnetic stirring for 6 hours to remove the iron. The solid sample was washed in succession with 2×100 mL water and 50 mL acetone under vacuum filtration over a PTFE membrane with pore size of 0.22 μm. Finally, the sample was dried at 70 °C in a vacuum oven for 1 hour to obtain the final material.

Characterization

The scanning electron microscopy (SEM) measurements were performed on a Hitachi S-4800 Scanning Electron Microscope operated at 15 kV. The samples were spray-coated with a thin layer of platinum before observation. The transmission electron microscopy (TEM) images and selected area electron diffraction (SAED) patterns were obtained on TEM JeoL-2100F with an accelerating voltage of 200 kV. The sample was dispersed in acetone with the aid of sonication and dropped on an amorphous carbon film supported on copper grid for TEM analysis. Powder XRD patterns were recorded on Rigaku D/max-2500 X-ray diffractometer using Cu-Kα radiation (λ=0.15406 nm) at a scanning rate of 8 degree per minute. The tube voltage was 40 kV and the current was 200 mA. The Raman spectra were recorded on a LabRAM ARAMIS Raman Microscope with an Nd/YAG laser (532 nm) at room

temperature. Scans were taken on an extended range (100-4000 cm^{-1}) and the exposure time was 50 s. The material was sonicated in acetone and dropped on to a silicon wafer with a thickness of 300 nm silicon oxide layer. The sample was viewed using a green laser apparatus under a magnification of ×50. The X-ray photoelectron spectroscopy (XPS) data were obtained with a Thermo ESCALab250 xi electron spectrometer from Thermo Scientific using 300 W Al-Kα radiation. The base pressure was about 1.68×10^{-9} mbar. The binding energies were referenced to the C1s line at 284.8 eV from adventitious carbon. The contents of elements in the samples were determined by ICP-AES (VISTAMPX).

Conductivity measurement

The product was milled and subsequently pressurized (10 MPa) to prepare the square pellet with 90 μm in thickness (d). The sheet resistance (R) of the powder sample was measured by Keithley 2000 Multimeter (Keithley Instruments Inc, USA) using a four point configuration method. The conductivity was calculated from the equation of $\sigma = 1/(R\times d)$.

Acknowledgements

The authors thank the financial supports from the National Natural Science Foundation of China (21133009, U1232203) and Chinese Academy of Sciences (KJCX2.YW.H30).

Notes and references

Beijing National Laboratory for Molecular Sciences, Institute of Chemistry, Chinese Academy of Sciences, Beijing 100190, China.
Tel/fax: 86-10-62562821. E-mail address: songjl@iccas.ac.cn; hanbx@iccas.ac.cn.

1 K. S. Novoselov, A. K. Geim, S. V. Morozov, D. Jiang, Y. Zhang, S. V. Dubonos, I. V. Grigorieva and A. A. Firsov, *Science*, 2004, **306**, 666.

2 (a) K. S. Novoselov, A. K. Geim, S. V. Morozov, D. Jiang, M. I. Katsnelson, I. V. Grigorieva, S. V. Dubonos and A. A. Firsov, *Nature*, 2005, **438**, 197; (b) Y. Zhang, Y. Tan, H. L. Stormer and P. Kim, *Nature*, 2005, **438**, 201; (c) D. Jariwala, V. K. Sangwan, L. J. Lauhon, T. J. Marks and M. C. Hersam, *Chem. Soc. Rev.*, 2013, **42**, 2824; (d) Y. N. Meng, Y. Zhao, C. G. Hu, H. H. Cheng, Y. Hu, Z. P. Zhang, G. Q. Shi and L. T. Qu, *Adv. Mater.*, 2013, **25**, 2326.

3 C. Lee, X. D. Wei, J. W. Kysar and J. Hone, *Science*, 2008, **321**, 385.

4 (a) K. Ellmer, *Nature Photon.*, 2012, **6**, 808; (b) M. Liu, X. Yin, E. Ulin-Avila, B. Geng, T. Zentgraf, L. Ju, F. Wang and X. Zhang, *Nature*, 2011, **474**, 64.

5 (a) A. A. Balandin, S. Ghosh, W. Bao, I. Calizo, D. Teweldebrhan, F. Miao and C. N. Lau, *Nano Lett.*, 2008, **8**, 902; (b) N. Savage, *Nature*, 2012, **483**, S30; (c) A. A. Balandin, *Nature Mater.*, 2011, **10**, 569.

6 K. S. Novoselov, V. I. Fal'ko, L. Colombo, P. R. Gellert, M. G. Schwab and K. Kim, *Nature*, 2012, **490**, 192.

7 (a) K. S. Kim, Y. Zhao, H. Jang, S. Y. Lee, J. M. Kim, K. S. Kim, J. Ahn, P. Kim, J. Choi and B. H. Hong, *Nature*, 2009, **457**, 706; (b) Y. Zhang, L. Y. Zhang and C. W. Zhou, *Acc. Chem. Res.*, 2013, **46**, 2329; (c) R. S. Edwards and K. S. Coleman, *Acc. Chem. Res.*, 2013, **46**, 23; (d) A. W. Tsen, L. Brown, R. W. Havener and J. Park, *Acc. Chem. Res.*, 2013, **46**, 2286.

8 D. A. C. Brownson, D. K. Kampouris and C. E. Banks, *Chem. Soc. Rev.*, 2012, **41**, 6944.

9 (a) C. Berger, Z. Song, X. Li, X. Wu, N. Brown, C. Naud, D. Mayou, T. Li, J. Hass, A. N. Marchenkov, E. H. Conrad, P. N. First and W. A. de Heer, *Science*, 2006, **312**, 1191; (b) B. Butz, C. Dolle, F. Niekiel, K. Weber, D. Waldmann, H. B. Weber, B. Meyer and E. Spiecker, *Nature*, 2014, **505**, 533; (c) D. Deng, X. Pan, H. Zhang, Q. Fu, D. Tan and X. Bao, *Adv. Mater.*, 2010, **22**, 2168.

10 (a) V. Georgakilas, M. Otyepka, A. B. Bourlinos, V. Chandra, N. Kim, K. C. Kemp, P. Hobza, R. Zboril and K. S. Kim, *Chem. Rev.*, 2012, **112**, 6156; (b) A. Hirsch, J. M. Englert and F. Hauke, *Acc. Chem. Res.*, 2013, **46**, 87; (c) A. Ciesielski and P. Samori, *Chem. Soc. Rev.*, 2014, **43**, 381.

11 Y. Hernandez, V. Nicolosi, M. Lotya, F. M. Blighe, Z. Sun, S. De, I. T. McGovern, B. Holland, M. Byrne, Y. K. Gun'Ko, J. Boland, P. Niraj, G. Duesberg, S. Krishnamurthy, R. Goodhue, J. Hutchison, V. Scardaci, A. C. Ferrari and J. N. Coleman, *Nature Nanotechnol.*, 2008, **3**, 563.

12 (a) S. Park and R. S. Ruoff, *Nature Nanotechnol.*, 2009, **4**, 217; (b) C. K. Chua and M. Pumera, *Chem. Soc. Rev.*, 2014, **43**, 291; (c) R. Larciprete, S. Fabris, T. Sun, P. Lacovig, A. Baraldi and S. Lizzit, *J. Am. Chem. Soc.*, 2011, **133**, 17315; (d) X. S. Zhou, T. B. Wu, K. L. Ding, B. J. Hu, M. Q. Hou and B. X. Han, *Chem. Commun.*, 2010, **46**, 386.

13 (a) X. H. Li, S. Kurasch, U. Kaiser and M. Antonietti, *Angew. Chem. Int. Ed.*, 2012, **51**, 9689; (b) A. Golzhauser, *Angew. Chem. Int. Ed.*, 2012, **51**, 10936; (c) K. V. Manukyan, S. Rouvimou, E. E. Wolf and A. S. Mukasyan, *Carbon*, 2013, **62**, 302.

14 M. Choucair, P. Thordarson and J. A. Stride, *Nature Nanotechnol.*, 2009, **4**, 30.

15 (a) C. D. Liao, Y. Y. Lu, S. R. Tamalampudi, H. C. Cheng and Y. T. Chen, *J. Phys.Chem. A*, 2013, **117**, 9454; (b) A. C. Ferrari and D. M. Basko, *Nature Nanotechnol.*, 2013, **8**, 235.

16 (a) X. Cao, D. Qi, S. Yin, J. Bu, F. Li, C. F. Goh, S. Zhang and X. Chen, *Adv. Mater.*, 2013, **25**, 2957; (b) I. K. Moon, J. Lee, R. S. Ruoff and H. Lee, *Nature Commun.*, 2010, **1**, 73.

17 J. E. Proctor, E. Gregoryanz, K. S. Novoselov, M. Lotya, J. N. Coleman and M. P. Halsall, *Phys. Rev. B*, 2009, **80**, 073408.

18 Z. Chen,W. Ren, L. Gao, B. Liu, S. Pei and H. Cheng, *Nature Mater.*, 2011, **10**, 424.

19 P. L. Walker, J. F. Rakszawski and A. F. Amington, *ASTM Bull.*, 1955, **208**, 52.

20 J. Lee, S. Kim, J. Yoon and J. Jang, *ACS Nano*, 2013, **7**, 6047.

21 X. Zhang, A. Hsu, H. Wang, Y. Song, J. Kong, M. S. Dresselhaus and T. Palacios, *ACS Nano*, 2013, **7**, 7262.

22 V. H. Pham, S. H. Hur, E. J. Kim, B. S. Kim and J. S. Chung, *Chem. Commun.*, 2013, **49**, 6665.

23 X. Z. Zhou, F. Boey and H. Zhang, *Chem. Soc. Rev.*, 2011, **40**, 5221.